PERGAMON

International Journal of Solids and Structures 37 (2000) 2727–2751

INTERNATIONAL JOURNAL OF SOLIDS and STRUCTURES

www.elsevier.com/locate/ijsolstr

Hybrid method for stress analysis of finite three-dimensional elastic components

Xin-Lin Gao [a,*], Robert E. Rowlands [b]

[a] *Department of Aeronautics and Astronautics, Air Force Institute of Technology, 2950 P Street, Wright–Patterson Air Force Base, OH 45433-7765, USA*

[b] *Department of Mechanical Engineering, University of Wisconsin–Madison, 1513 University Avenue, Madison, WI 53706-1572, USA*

Received 15 August 1998; in revised form 30 March 1999

Abstract

A new hybrid experimental–analytical/numerical method for stress analysis of a finite three-dimensional elastic component is developed in this paper. It uses the experimentally measured surface stresses and a Green's function method to determine the displacement field (and thus strain and stress fields) in the interior of the component. The method is based on a displacement formulation in three-dimensional elasticity. It is first demonstrated that solving the elasticity problem can be reduced to solving two kinds of Dirichlet problems of Laplace and Poisson equations when the surface stresses become known. These Dirichlet problems are then solved by using Green's function method in potential theory. The solutions are derived in integral forms in terms of the Green function, which is unique for given shape of the engineering component. Green's functions for three typical shapes of a rectangular prism, a solid cylinder and a solid sphere are provided. A sample problem is analyzed to demonstrate applications of the new method. The present method differs from the known boundary integral equation method in elasticity theory. In addition, it can be directly applied to actual engineering components, unlike the model-based photoelasticity method.

1. Introduction

Many problems in engineering practice involve the determination of stresses and/or displacements in bodies that are three-dimensional. Exact analytical solutions are available only for a few three-dimensional problems with simple geometries and/or loading conditions. Hence, numerical or experimental analyses are generally required in solving such problems. Numerical solutions by themselves can be erroneous. On the other hand, photoelasticity is the only developed experimental method of three-dimen-

* Corresponding author. Fax: +001-937-656-7621.

0020-7683/00/$ - see front matter
PII: S0020-7683(99)00111-0

sional stress analysis. However, this method is not very convenient to use since it typically necessitates loading a prepared plastic model to 'freeze' the stresses and subsequently analyzing slices removed from the model.

To overcome the difficulties inherent in analytical, numerical or experimental procedures, hybrid experimental–analytical/numerical stress analysis has emerged as an alternative approach. Hybrid techniques synergize the merits of individual analytical, numerical and experimental methods. One hybrid method typically involves measuring stress, strain or displacement data on the entire boundary of an engineering component in the first place. Then, the governing equations in conjunction with the experimentally measured boundary conditions, some of which might be superfluous, are solved by using suitable analytical/numerical methods to determine the stress, strain and displacement fields throughout the interior of the component. The successful use of a hybrid method can thereby reduce the amount of measurements required, increase the accuracy of numerical results and, at the same time, enable the expeditious determination of the complete stress, strain and displacement distributions throughout the component.

The use of hybrid experimental–numerical methods is quite recent. Jacob's dissertation appears to be the first systematic development of three-dimensional hybrid stress analysis (Jacob, 1976). The major part of this work was reported in Chandrashekhara and Jacob (1977a, 1977b). Barishpolsky (1980, 1981) presented a somewhat different formulation of this hybrid method. He used generalized curvilinear coordinates in an attempt to make the method applicable for a three-dimensional body of arbitrary shape. Rao (1982) extended the work of Chandrashekhara and Jacob (1977a, 1977b) further to include body forces and thermal loads. In all of these studies mentioned above a photoelastic model and the stress freezing technique are used to determine surface stresses at discrete points, and a finite difference method is employed to solve the Beltrami–Michell compatibility equations. Although serious efforts were made by the authors to justify/interpret their numerical results, there exists a fundamental concern with their approach. These authors treated the six Beltrami–Michell compatibility equations as independent expressions to solve for the six unknown stress components. This is conceptually incomplete because the six second-order compatibility equations are only equivalent to three independent fourth-order partial differential equations (see a proof provided in Appendix A). These three fourth-order equations, together with the three equilibrium equations, consist of the six independent equations to solve for the six unknown stress components (see, for example, Chou and Pagano, 1967, p.79). Hence, such analyses warrant strengthening.

Laermann (1984a, 1984b, 1990) has proposed an alternative hybrid procedure utilizing holographically measured displacements at discrete points on the surface and an approximate method based on Taylor's series to solve the Navier equations for the displacements at interior points of a three-dimensional elastic component. The accuracy of this method could probably be improved by not truncating the series involved after the fourth term.

In this paper, a new hybrid method is developed. It uses the measured surface stresses and a Green's function method to determine the displacement field (and thus strain and stress fields) in the interior of a three-dimensional elastic component. In Section 2, the basic governing equations and the two formulation methods in three-dimensional elasticity are reviewed and compared, which leads to the adoption of a displacement approach in formulating the new method. Section 3 presents the formulation of the new hybrid method. The formulation provided is general and valid for finite three-dimensional domains of arbitrary shape. In Section 4, the sample problem of an elastic cube subjected to hydrostatic pressure is analyzed to demonstrate applications of the new method. A summary is provided in Section 5.

2. Review of governing equations in elasticity

The basic governing equations of the three-dimensional linear elasticity in the usual Cartesian coordinates $\{x_1, x_2, x_3\} \equiv \{x, y, z\}$ are the equilibrium equations (in the absence of body forces)

$$\sigma_{ij,j} = 0, \tag{1}$$

the constitutive equations

$$\sigma_{ij} = 2\mu\varepsilon_{ij} + \lambda\varepsilon_{kk}\delta_{ij}, \tag{2}$$

the geometrical (strain–displacement) equations

$$\varepsilon_{ij} = \frac{1}{2}(u_{i,j} + u_{j,i}) \tag{3}$$

and the compatibility equations

$$\varepsilon_{ik,jj} - \varepsilon_{jk,ij} + \varepsilon_{jj,ik} - \varepsilon_{ij,jk} = 0. \tag{4}$$

Eq. (2) may also be written as

$$\varepsilon_{ij} = \frac{1}{E}[(1+\nu)\sigma_{ij} - \nu S\delta_{ij}], \tag{5}$$

where

$$S \equiv \sigma_{kk} = \sigma_{xx} + \sigma_{yy} + \sigma_{zz} \tag{6}$$

is the first stress invariant. In the above equations, σ_{ij}, ε_{ij} and u_i are, respectively, the Cartesian stress, strain and displacement components; δ_{ij} is the Kronecker delta; E and ν are Young's modulus and Poisson's ratio, respectively; and μ and λ are the Lame constants, with

$$\mu = \frac{E}{2(1+\nu)} \tag{7a}$$

and

$$\lambda = \frac{2\nu\mu}{1-2\nu}. \tag{7b}$$

As usual, Einstein's summation convention applies and the indices i, j, k, etc. range over $\{1, 2, 3\}$.

Note that in a stress formulation Eqs. (1), (4) and (5) are essential while, in a displacement formulation, Eqs. (1)–(3) must be satisfied.

First, we consider a stress formulation. Using Eqs. (1) and (5) in Eq. (4) and carrying out the index operations will result in (see, for example, Chou and Pagano, 1967)

$$\Delta\sigma_{ij} + \frac{1}{1+\nu}S_{,ij} = 0, \tag{8}$$

where Δ is the Laplace operator. The expressions given by Eq. (8), which represent the six compatibility equations in terms of stress, are known as the Beltrami–Michell compatibility equations. Since the six equations listed in Eq. (4) are equivalent to only three independent fourth-order equations (see a proof in Appendix A) and the operations that lead to Eq. (8) from Eq. (4) are linear, it follows that the six

equations given by Eq. (8) amount to only three independent fourth-order equations. That is, the Beltrami–Michell compatibility equations given by Eq. (8) alone are not sufficient to solve for the six unknown stress components. It is therefore believed that those analyses by Chandrashekhara and Jacob (1977a, 1977b) and their followers are unfortunately incorrect, as mentioned in Section 1. The six compatibility equations given by Eq. (8) (or their three fourth-order equivalents) and the three equilibrium equations listed in Eq. (1), in conjunction with suitable stress boundary conditions, define the boundary-value problem to solve for the six stress components throughout a three-dimensional elastic member. In some special cases, this boundary-value problem may be exactly solved by using a stress function method (see, for example, Chou and Pagano, 1967, pp. 277–282; Little, 1973, pp. 317–320). However, it is very difficult to solve such problems analytically if they involve finite geometry.

We now examine a displacement formulation. Inserting Eqs. (2) and (3) into Eq. (1) and using Eqs. (7a) and (7b) will yield

$$\Delta u_i + \frac{1}{1-2\nu} e_{,i} = 0, \tag{9}$$

where

$$e \equiv \varepsilon_{kk} = \varepsilon_{xx} + \varepsilon_{yy} + \varepsilon_{zz} = u_{k,k} \tag{10}$$

is the first strain invariant. The expressions given by Eq. (9), which represent the three equilibrium equations in terms of displacement, are known as the Navier equations. Taking the divergence of Eq. (9) and using Eq. (10) will give

$$\Delta e = 0. \tag{11}$$

Clearly, Eq. (11) is a necessary condition for Eq. (9) and hence is always true for any three-dimensional elastic component in equilibrium. Moreover, taking the trace of Eq. (2) and invoking Eqs. (6), (7) and (10) will lead to

$$S = \frac{E}{1-2\nu} e. \tag{12}$$

Substituting Eq. (12) into Eq. (11) then gives

$$\Delta S = 0. \tag{13}$$

Note that Eq. (11) is a Laplace equation. Once e has been determined, the Navier equations given by Eq. (9) will become three decoupled Poisson's equations. Hence, if the displacement vector (and thus e from Eq. (10)) can be determined on the entire surface, then Eqs. (9) and (11) can be solved to obtain the interior displacement field using a variety of methods in potential theory, a well-studied discipline in applied mathematics (see, for example, Kellogg, 1953; Sneddon, 1966).

Finally, note that the system of Eqs. (1) and (8) can be written in a tensorial form as

$$\underline{\nabla} \cdot \underline{\sigma} = \underline{0}, \tag{14a}$$

$$\Delta \underline{\sigma} + \frac{1}{1+\nu} \underline{\nabla}(\underline{\nabla} S) = \underline{0}, \tag{14b}$$

where $\underline{\sigma}$ is the stress tensor, $\underline{\nabla}$ is the gradient operator and $\underline{\nabla}\cdot$ is the divergence operator. Similarly, Eq. (9) can be written as

$$\Delta \underline{u} + \frac{1}{1-2\nu}\underline{\nabla} e = \underline{0}, \tag{15}$$

where $\underline{u}$ is the displacement vector. Eqs. (14a), (14b) and (15) are coordinate-free and valid for any curvilinear coordinate system, while Eqs. (1), (8) and (9) are only applicable for the Cartesian coordinate system $\{x_1, x_2, x_3\} \equiv \{x, y, z\}$.

Eqs. (14a) and (14b) represent the most general form of the governing equations of the three-dimensional elasticity in a stress formulation, and Eq. (15) in a displacement formulation. A comparison shows that the system defined in Eq. (15) is much easier to solve than that defined in Eqs. (14a) and (14b) if one can determine $\underline{u}$ on the entire surface of the body and decouple the three equations in Eq. (15). This motivates us to adopt a displacement formulation in the next section.

3. New hybrid method

In a displacement formulation using the Cartesian coordinates $\{x_1, x_2, x_3\}$, one only needs to solve Eq. (9) subject to suitable boundary conditions. Since Eq. (11), as a necessary condition of Eq. (9), always holds, one can solve it to obtain e throughout a loaded three-dimensional elastic component in the first place. This will decouple the three Navier equations given by Eq. (9) and convert them into three independent Poisson's equations, which are much easier to solve.

3.1. Determination of the first strain invariant e

Note that e can be easily obtained from Eq. (12) once S has been determined from Eq. (13) and the associated boundary conditions.

Since it has been proven that the elasticity solution for any determinate problem is unique (see, for example, Sokolnikoff, 1956; Chou and Pagano, 1967, pp. 82–84), Eq. (13) must also have a unique solution. From potential theory, Laplace's and Poisson's equations subject to Dirichlet boundary conditions (as sufficient conditions) have unique solutions. Therefore, for Eq. (13) to have a unique solution, it is sufficient to have the first stress invariant, S, known on the entire surface. However, Cauchy's principle of stress (see, for example, Malvern, 1969, pp. 64–119) enables one to determine only three stress components (one normal stress and two shear stresses) from the known tractions on any part of the surface. Hence, an appropriate experimental measurement is required in the first place to obtain the other three surface stress components.

Current developments (see, for example, Barone et al., 1998) of a new experimental stress analysis method which combines the thermal stress analysis (TSA) (see, for example, Rauch and Rowlands, 1993) and the birefringent coating (see, for example, Zandman et al., 1977; Rowlands, 1981; Lesniak et al., 1997) techniques will enable the determination of all six stress components on the surface of an elastic solid. Then, Eq. (13) and the experimentally measured S on the surface form the standard Dirichlet problem:

$$\Delta S = 0 \text{ in } \Omega, \tag{16a}$$

$$S = S^* \text{ on } \Gamma, \tag{16b}$$

where Ω denotes the interior of the three-dimensional elastic member, Γ the surface of the member; and

S^* is the measured distribution of S on Γ. This boundary-value problem can be solved using a Green's function method (see, for example, Stakgold, 1979) as follows.

Note that Green's function associated with the Dirichlet problem (16a) and (16b) is defined by the boundary-value problem:

$$\Delta G = \delta(\underline{x} - \underline{\xi}) \text{ in } \Omega, \tag{17a}$$

$$G = 0 \text{ on } \Gamma, \tag{17b}$$

where $G \equiv G(\underline{x}, \underline{\xi})$ is Green's function, δ is the Dirac delta function, $\underline{x} = x_i \underline{e}_i$ is the position vector of a typical point in Ω, and $\underline{\xi} = \xi_i \underline{e}_i$ is the location of the source point.

Using Green's second identity (see, for example, Flanigan, 1972, p. 62) for this case:

$$\int_\Omega (S\Delta G - G\Delta S)\mathrm{d}V_{\underline{x}} = \int_\Gamma \left(S\frac{\partial G}{\partial n_{\underline{x}}} - G\frac{\partial S}{\partial n_{\underline{x}}} \right) \mathrm{d}A_{\underline{x}} \tag{18}$$

gives, after substituting Eqs. (16a), (16b), (17a) and (17b) and interchanging the roles of $\underline{x}$ and $\underline{\xi}$,

$$S(\underline{x}) = \int_\Gamma S^*(\underline{\xi}) \frac{\partial G(\underline{\xi}, \underline{x})}{\partial n_{\underline{\xi}}} \, \mathrm{d}A_{\underline{\xi}} \tag{19}$$

as the unique solution of Eqs. (16a) and (16b), where the subscript $\underline{\xi}$ denotes integration with respect to $\underline{\xi} = \xi_i \underline{e}_i$. Substituting Eq. (19) into Eq. (12) then yields

$$e(\underline{x}) = \frac{1 - 2\nu}{E} \int_\Gamma S^*(\underline{\xi}) \frac{\partial G(\underline{\xi}, \underline{x})}{\partial n_{\underline{\xi}}} \, \mathrm{d}A_{\underline{\xi}} \tag{20}$$

as the first strain invariant at any point $\underline{x}$ in Ω in terms of Green's function $G(\underline{x}, \underline{\xi})$ defined by Eqs. (17a) and (17b).

Since both e and S are invariant under coordinate transformations, the solution given by Eq. (20) is valid for any coordinate system.

3.2. Solution for the displacement vector $\underline{u}$

Note that once $e(\underline{x})$ is known, the three equations given by Eq. (9) become decoupled and hence can be solved separately.

From Eq. (5), the strain components on the surface Γ, ε_{ij}^*, are related to the measured surface stress components σ_{ij}^* by

$$\varepsilon_{ij}^* = \frac{1}{E}\left[(1 + \nu)\sigma_{ij}^* - \nu S^* \delta_{ij}\right]. \tag{21}$$

Since ε_{ij}^* are obtained directly from the physically measured σ_{ij}^*, they must automatically satisfy the compatibility equations given by Eq. (4). Hence, the displacement components on the surface can be determined from ε_{ij}^* as (see, for example, Love, 1944, pp. 222–223; Malvern, 1969, pp. 188–192)

$$u_i^*(\underline{x}) = u_i^*(\underline{x}^0) + \left(x_j - x_j^0\right)\omega_{ij}^*(\underline{x}^0) + \int_C \left[\varepsilon_{ij}^* + (\xi_k - x_k)\left(\frac{\partial \varepsilon_{ji}^*}{\partial \xi_k} - \frac{\partial \varepsilon_{kj}^*}{\partial \xi_i} \right) \right] \mathrm{d}\xi_j, \tag{22}$$

where $\underline{x}$ and $\underline{x}^0$ are, respectively, a typical (arbitrary) point and a chosen (convenient) point on the surface Γ, C is an arbitrary (convenient) path connecting $\underline{x}$ and $\underline{x}^0$ on Γ, and ω_{ij}^* are the components of the rotation tensor. Clearly, the first two terms in Eq. (22) represent the effects of a rigid-body motion and will not contribute to the stress and strain fields. Hence, they can be suppressed without violating any (stress) boundary conditions and the stress and strain distributions. Then, the surface displacement components u_i^* will be solely determined from ε_{ij}^*. Eq. (22) provides the general formulae to determine u_i^* from the surface strains ε_{ij}^*, which can be used for all cases. In practice, however, the determination of u_i^* from known ε_{ij}^* can often be carried out more conveniently by direct integration rather than making specific use of Eq. (22) (see, for example, Malvern, 1969, pp. 190–192; Gao, 1999), since the integrability of each strain–displacement relation is guaranteed by the fact that the compatibility equations are satisfied by ε_{ij}^*.

Knowing both $e(\underline{x})$ and u_i^* (from the measured surface stresses), one then obtains from Eq. (9) and the boundary conditions that

$$\Delta u_i = -\frac{1}{1-2\nu} e_{,i} \text{ in } \Omega, \tag{23a}$$

$$u_i = u_i^* \text{ on } \Gamma. \tag{23b}$$

These are now three separate Dirichlet problems of Poisson's equation to solve for u_i ($i = \{1, 2, 3\}$). Note that Eqs. (23a) and (23b) can be decomposed into the following two boundary-value problems:

$$\Delta u_i = -\frac{1}{1-2\nu} e_{,i} \text{ in } \Omega, \tag{24a}$$

$$u_i = 0 \text{ on } \Gamma \tag{24b}$$

and

$$\Delta u_i = 0 \text{ in } \Omega, \tag{25a}$$

$$u_i = u_i^* \text{ on } \Gamma. \tag{25b}$$

Following the same procedures as those used in solving Eqs. (16a) and (16b), the solution of Eqs. (25a) and (25b) is obtained as

$$u_i^{\mathrm{II}}(\underline{x}) = \int_\Gamma u_i^*(\underline{\xi}) \frac{\partial G(\underline{\xi},\underline{x})}{\partial n_{\underline{\xi}}} \, \mathrm{d}A_{\underline{\xi}}. \tag{26}$$

Using Green's second identity and Eqs. (24a), (24b), (17a) and (17b) will result in

$$u_i^{\mathrm{I}}(\underline{x}) = -\frac{1}{1-2\nu} \int_\Omega G(\underline{\xi},\underline{x}) \frac{\partial e(\underline{\xi})}{\partial \xi_i} \, \mathrm{d}V_{\underline{\xi}} \tag{27}$$

as the solution of the first boundary-value problem defined by Eqs. (24a) and (24b). Therefore, it follows from the principle of superposition that the solution of Eqs. (23a) and (23b) is

$$u_i(\underline{x}) = u_i^{\mathrm{I}}(\underline{x}) + u_i^{\mathrm{II}}(\underline{x}) = -\frac{1}{1-2\nu} \int_\Omega G(\underline{\xi},\underline{x}) \frac{\partial e(\underline{\xi})}{\partial \xi_i} \, \mathrm{d}V_{\underline{\xi}} + \int_\Gamma u_i^*(\underline{\xi}) \frac{\partial G(\underline{\xi},\underline{x})}{\partial n_{\underline{\xi}}} \, \mathrm{d}A_{\underline{\xi}}. \tag{28}$$

This gives the displacement components at any point $\underline{x}$ in Ω in terms of Green's function $G(\underline{x}, \underline{\xi})$ defined by Eqs. (17a) and (17b). By using Eq. (28), the strain and stress components at any point $\underline{x}$ in Ω can then be easily calculated from Eqs. (3) and (2), respectively.

In a tensorial form, Eq. (28) becomes

$$\underline{u}(\underline{x}) = -\frac{1}{1-2\nu}\int_{\Omega} G(\underline{\xi},\underline{x})\underline{\nabla}_{\underline{\xi}} e(\underline{\xi}) \mathrm{d}V_{\underline{\xi}} + \int_{\Gamma} \underline{u}^{*}(\underline{\xi}) \frac{\partial G(\underline{\xi},\underline{x})}{\partial n_{\underline{\xi}}} \mathrm{d}A_{\underline{\xi}}, \tag{29}$$

which is applicable for *any* coordinate system.

It is now clear that the three-dimensional elasticity problem defined in the finite domain $\Omega \cup \Gamma$, which is generic, will be completely solved once Green's function defined by Eqs. (17a) and (17b) has become available.

3.3. Green's function $G(\underline{x}, \underline{\xi})$ for a finite three-dimensional domain

3.3.1. Determination of $G(\underline{x}, \underline{\xi})$ from Green's function in unbounded 3-D space

Let

$$G = g + b, \tag{30}$$

where $b(\underline{x})$ is a function yet unknown, and $g(\underline{x}, \underline{\xi})$ is the Green function in the unbounded three-dimensional space given by (see, for example, Stakgold, 1979)

$$g = -\frac{1}{4\pi}\frac{1}{|\underline{x} - \underline{\xi}|} \tag{31}$$

and satisfying

$$\Delta g = \delta(\underline{x} - \underline{\xi}). \tag{32}$$

Using Eqs. (30) and (32) in Eqs. (17a) and (17b) then leads to

$$\Delta b = 0 \text{ in } \Omega,$$

$$b = -g|_{\Gamma} \text{ on } \Gamma. \tag{33}$$

The solution of this boundary-value problem gives $b(\underline{x})$, an harmonic function. Substituting this function and Eq. (31) into Eq. (30) then yields Green's function $G(\underline{x}, \underline{\xi})$ for the finite domain $\Omega \cup \Gamma$.

3.3.2. Determination of $G(\underline{x}, \underline{\xi})$ from solving simple Dirichlet problems of Poisson's equation

Consider the Dirichlet problem with homogeneous boundary conditions:

$$\Delta f = F(\underline{x}) \text{ in } \Omega,$$

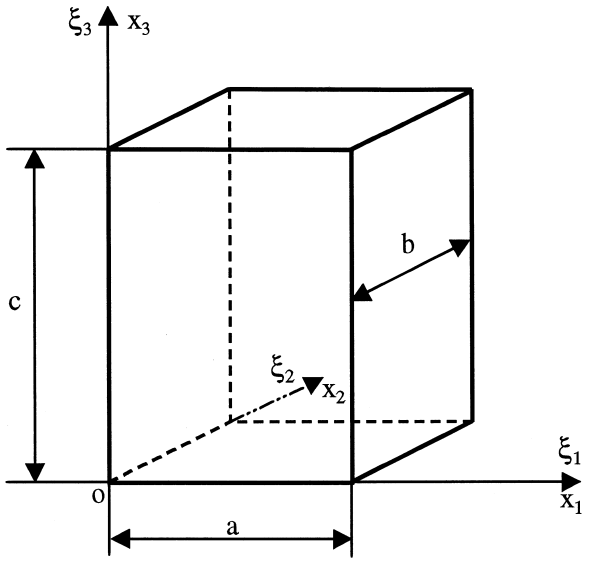

Fig. 1. Rectangular prism.

$$f = 0 \text{ on } \Gamma, \tag{34}$$

where $f(\underline{x})$ is the unknown function, and $F(\underline{x})$ is a given continuous function. Using Green's second identity and Eqs. (17a), (17b) and (34) gives

$$f(\underline{x}) = \int_{\Omega} G(\underline{\xi},\underline{x}) F(\underline{\xi}) \mathrm{d}V_{\underline{\xi}} \tag{35}$$

as the unique solution of Eq. (34). Hence, if one can solve Eq. (34) and express its solution in the form of Eq. (35), then Green's function $G(\underline{x}, \underline{\xi})$ can be directly read off from Eq. (35). This is a convenient

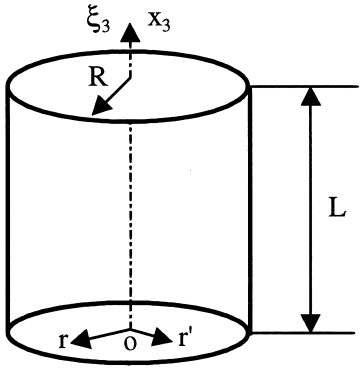

Fig. 2. Solid cylinder.

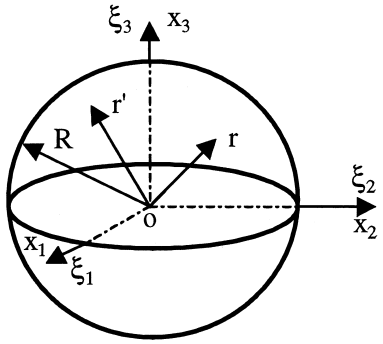

Fig. 3. Solid sphere.

method to derive Green's functions for standard three-dimensional domains such as parallelepipeds, cylinders and spheres by using the separation-of-variable method and a very simple function $F(\underline{x})$.

3.3.3. Green's function for a rectangular prism

For the prism with width a, length b and height c, as shown in Fig. 1, it can be shown (see Appendix B) that Green's function defined by Eqs. (17a) and (17b) is

$$G(\underline{x},\underline{\xi}) = -8\sum_{m=1}^{\infty}\sum_{n=1}^{\infty}\sum_{p=1}^{\infty}\frac{1}{\pi^2 abc\left(\frac{m^2}{a^2}+\frac{n^2}{b^2}+\frac{p^2}{c^2}\right)}\sin\frac{m\pi x_1}{a}\sin\frac{m\pi\xi_1}{a}\sin\frac{n\pi x_2}{b}\sin\frac{n\pi\xi_2}{b}$$
$$\times\sin\frac{p\pi x_3}{c}\sin\frac{p\pi\xi_3}{c}, \tag{36}$$

where $\underline{x}=(x_1, x_2, x_3)$ is a typical point in the prism, and $\underline{\xi}=(\xi_1, \xi_2, \xi_3)$ is the source point.

3.3.4. Green's function for a solid cylinder

For the solid cylinder of radius R and length L, as shown in Fig. 2, Green's function defined by Eqs. (17a) and (17b) is obtained (see Appendix B) as

$$G(\underline{x},\underline{\xi}) = -\sum_{m=1}^{\infty}\sum_{n=1}^{\infty}\frac{2}{\pi R^2 L\left[\left(\frac{\beta_m}{R}\right)^2+\left(\frac{n\pi}{L}\right)^2\right]}\frac{J_0\left(\beta_m\frac{r}{R}\right)J_0\left(\beta_m\frac{r'}{R}\right)}{J_1^2(\beta_m)}\sin\frac{n\pi x_3}{L}\sin\frac{n\pi\xi_3}{L}, \tag{37}$$

where $\underline{x}=r\underline{e}_\theta+x_3\underline{e}_3$ is a typical point in the cylinder, $\underline{\xi}=r'\underline{e}_\theta+\xi_3\underline{e}_3$ is the source point, J_0 and J_1 are, respectively, the first-kind Bessel functions of order zero and one, and β_m (m = 1, 2, 3,...) are the dimensionless eigenvalues (roots) found from $J_0(\beta_m)=0$.

3.3.5. Green's function for a solid sphere

For the solid sphere of radius R, as shown in Fig. 3, Green's function defined by Eqs. (17a) and (17b)

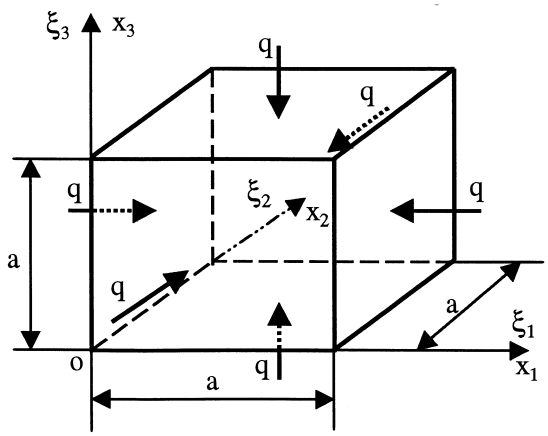

Fig. 4. Cube subjected to hydrostatic pressure.

can be shown to be (see Appendix B)

$$G(\underline{x},\underline{\xi}) = -\sum_{m=1}^{\infty} \frac{R}{2\pi^3 r r' m^2} \sin\frac{m\pi r}{R} \sin\frac{m\pi r'}{R}, \tag{38}$$

where $\underline{x} = r\underline{e}_R$ is a typical point in the sphere, and $\underline{\xi} = r'\underline{e}_R$ is the source point.

Since these three standard domains and their combinations represent many load-carrying engineering components and structures, the Green functions provided here should be able to account for many important practical cases.

4. An example

A sample problem is analyzed in this section to illustrate the hybrid method developed in the preceding section. Since the details of the new experimental stress analysis method mentioned in Section 3.1 are still under development and no measured full-field, three-dimensional surface stress data are available yet, the sample problem to be analyzed here is chosen in such a way that its closed-form solution is known and the needed full-field surface data can be easily obtained from the solution.

Consider the problem of an elastic cube with side length a and subjected to hydrostatic pressure q, as illustrated in Fig. 4. The exact solution of this problem is known to be

$$\sigma_{11} = \sigma_{22} = \sigma_{33} = -q, \quad \sigma_{12} = \sigma_{23} = \sigma_{31} = 0 \tag{39}$$

at any $\underline{x} \in \Omega \cup \Gamma$. It then follows from Eqs. (6) and (39) that

$$S^*(\underline{x}) = -3q \tag{40}$$

on the entire surface (i.e., for all $\underline{x} \in \Gamma$). Also, using Eq. (39) in Eq. (5) yields

$$\varepsilon_{11} = \varepsilon_{22} = \varepsilon_{33} = -\frac{q(1-2\nu)}{E}, \quad \varepsilon_{12} = \varepsilon_{23} = \varepsilon_{31} = 0 \tag{41}$$

at any $\underline{x} \in \Omega \cup \Gamma$. It can be shown (see Appendix C) that the three displacements (with the rigid-body motion suppressed) can be determined from the six strain components listed in Eq. (41) as

$$u_1(\underline{x}) = -\frac{q(1-2\nu)}{E}x_1, \quad u_2(\underline{x}) = -\frac{q(1-2\nu)}{E}x_2, \quad u_3(\underline{x}) = -\frac{q(1-2\nu)}{E}x_3 \tag{42}$$

at any point $\underline{x} \in \Omega \cup \Gamma$. In particular, on the surface (six faces) of the cube, Eq. (42) gives

$$u_1 = 0, \quad u_2 = -\frac{q(1-2\nu)}{E}x_2, \quad u_3 = -\frac{q(1-2\nu)}{E}x_3 \text{ on } x_1 = 0;$$

$$u_1 = -\frac{q(1-2\nu)}{E}a, \quad u_2 = -\frac{q(1-2\nu)}{E}x_2, \quad u_3 = -\frac{q(1-2\nu)}{E}x_3 \text{ on } x_1 = a;$$

$$u_1 = -\frac{q(1-2\nu)}{E}x_1, \quad u_2 = 0, \quad u_3 = -\frac{q(1-2\nu)}{E}x_3 \text{ on } x_2 = 0;$$

$$u_1 = -\frac{q(1-2\nu)}{E}x_1, \quad u_2 = -\frac{q(1-2\nu)}{E}a, \quad u_3 = -\frac{q(1-2\nu)}{E}x_3 \text{ on } x_2 = a;$$

$$u_1 = -\frac{q(1-2\nu)}{E}x_1, \quad u_2 = -\frac{q(1-2\nu)}{E}x_2, \quad u_3 = 0 \text{ on } x_3 = 0;$$

$$u_1 = -\frac{q(1-2\nu)}{E}x_1, \quad u_2 = -\frac{q(1-2\nu)}{E}x_2, \quad u_3 = -\frac{q(1-2\nu)}{E}a \text{ on } x_3 = a. \tag{43}$$

Next, we will apply the hybrid method developed in Section 3 to demonstrate that the displacements in the interior of the cube, as given by Eq. (42), are obtainable from the surface data listed in Eqs. (40) and (43) and the Green function given by Eq. (36).

Note that from the expression of Green's function given by Eq. (36) it follows, for the present case with $a = b = c$, that

$$\left.\frac{\partial G(\underline{\xi},\underline{x})}{\partial n_{\underline{\xi}}}\right|_{\xi_1=0} = 8\sum_{m=1}^{\infty}\sum_{n=1}^{\infty}\sum_{p=1}^{\infty}\frac{\sin\dfrac{m\pi x_1}{a}\sin\dfrac{n\pi x_2}{a}\sin\dfrac{p\pi x_3}{a}}{\pi^2 a(m^2+n^2+p^2)}\frac{m\pi}{a}\sin\frac{n\pi\xi_2}{a}\sin\frac{p\pi\xi_3}{a},$$

$$\left.\frac{\partial G(\underline{\xi},\underline{x})}{\partial n_{\underline{\xi}}}\right|_{\xi_1=a} = -8\sum_{m=1}^{\infty}\sum_{n=1}^{\infty}\sum_{p=1}^{\infty}\frac{\sin\dfrac{m\pi x_1}{a}\sin\dfrac{n\pi x_2}{a}\sin\dfrac{p\pi x_3}{a}}{\pi^2 a(m^2+n^2+p^2)}\frac{m\pi}{a}(-1)^m\sin\frac{n\pi\xi_2}{a}\sin\frac{p\pi\xi_3}{a},$$

$$\left.\frac{\partial G(\underline{\xi},\underline{x})}{\partial n_{\underline{\xi}}}\right|_{\xi_2=0} = 8\sum_{m=1}^{\infty}\sum_{n=1}^{\infty}\sum_{p=1}^{\infty}\frac{\sin\frac{m\pi x_1}{a}\sin\frac{n\pi x_2}{a}\sin\frac{p\pi x_3}{a}}{\pi^2 a(m^2+n^2+p^2)}\frac{n\pi}{a}\sin\frac{m\pi\xi_1}{a}\sin\frac{p\pi\xi_3}{a},$$

$$\left.\frac{\partial G(\underline{\xi},\underline{x})}{\partial n_{\underline{\xi}}}\right|_{\xi_2=a} = -8\sum_{m=1}^{\infty}\sum_{n=1}^{\infty}\sum_{p=1}^{\infty}\frac{\sin\frac{m\pi x_1}{a}\sin\frac{n\pi x_2}{a}\sin\frac{p\pi x_3}{a}}{\pi^2 a(m^2+n^2+p^2)}\frac{n\pi}{a}(-1)^n\sin\frac{m\pi\xi_1}{a}\sin\frac{p\pi\xi_3}{a},$$

$$\left.\frac{\partial G(\underline{\xi},\underline{x})}{\partial n_{\underline{\xi}}}\right|_{\xi_3=0} = 8\sum_{m=1}^{\infty}\sum_{n=1}^{\infty}\sum_{p=1}^{\infty}\frac{\sin\frac{m\pi x_1}{a}\sin\frac{n\pi x_2}{a}\sin\frac{p\pi x_3}{a}}{\pi^2 a(m^2+n^2+p^2)}\frac{p\pi}{a}\sin\frac{m\pi\xi_1}{a}\sin\frac{n\pi\xi_2}{a},$$

$$\left.\frac{\partial G(\underline{\xi},\underline{x})}{\partial n_{\underline{\xi}}}\right|_{\xi_3=a} = -8\sum_{m=1}^{\infty}\sum_{n=1}^{\infty}\sum_{p=1}^{\infty}\frac{\sin\frac{m\pi x_1}{a}\sin\frac{n\pi x_2}{a}\sin\frac{p\pi x_3}{a}}{\pi^2 a(m^2+n^2+p^2)}\frac{p\pi}{a}(-1)^p\sin\frac{m\pi\xi_1}{a}\sin\frac{n\pi\xi_2}{a}. \tag{44}$$

Using Eqs. (40) and (44) in Eq. (20) and carrying out the algebra will lead to

$$e(\underline{x}) = -\frac{3(1-2\nu)q}{E}\sum_{m=1}^{\infty}\sum_{n=1}^{\infty}\sum_{p=1}^{\infty}[1-(-1)^m][1-(-1)^n][1-(-1)^p]\frac{8\sin\frac{m\pi x_1}{a}\sin\frac{n\pi x_2}{a}\sin\frac{p\pi x_3}{a}}{\pi^3 mnp} \tag{45}$$

at any $\underline{x}\in\Omega$.

Note that from the Fourier analysis,

$$\sum_{l=1}^{\infty}\frac{2}{l\pi}[1-(-1)^l]\sin\frac{l\pi x_i}{a} \equiv 1 \text{ on } x_i\in[0,a]. \tag{46}$$

Then, using Eq. (46) in Eq. (45) yields

$$e(\underline{x}) = \frac{1-2\nu}{E}(-3q),\ \forall\underline{x}\in\Omega. \tag{47}$$

Substituting Eqs. (36), (43), (44) and (47) into Eq. (28) results in, after the algebra,

$$u_1(\underline{x}) = \frac{q(1-2\nu)}{E}\sum_{m=1}^{\infty}\sum_{n=1}^{\infty}\sum_{p=1}^{\infty}(-1)^m[1-(-1)^n][1-(-1)^p]\frac{8a\sin\frac{m\pi x_1}{a}\sin\frac{n\pi x_2}{a}\sin\frac{p\pi x_3}{a}}{\pi^3 mnp},$$

$$u_2(\underline{x}) = \frac{q(1-2\nu)}{E}\sum_{m=1}^{\infty}\sum_{n=1}^{\infty}\sum_{p=1}^{\infty}(-1)^n[1-(-1)^m][1-(-1)^p]\frac{8a\sin\frac{m\pi x_1}{a}\sin\frac{n\pi x_2}{a}\sin\frac{p\pi x_3}{a}}{\pi^3 mnp},$$

$$u_3(\underline{x}) = \frac{q(1-2\nu)}{E}\sum_{m=1}^{\infty}\sum_{n=1}^{\infty}\sum_{p=1}^{\infty}(-1)^p[1-(-1)^m][1-(-1)^n]\frac{8a\sin\frac{m\pi x_1}{a}\sin\frac{n\pi x_2}{a}\sin\frac{p\pi x_3}{a}}{\pi^3 mnp} \tag{48}$$

at any $\underline{x}\in\Omega$. From the Fourier analysis,

$$\sum_{l=1}^{\infty}\frac{-2a}{l\pi}(-1)^l\sin\frac{l\pi x_i}{a} \equiv x_i \text{ on } x_i\in[0,a]. \tag{49}$$

With the substitution of Eqs. (46) and (49), Eq. (48) then reduces to

$$u_i(\underline{x}) = -\frac{q(1-2\nu)}{E}x_i,\ \forall\underline{x}\in\Omega. \tag{50}$$

Clearly, the expressions of the three displacement components given by Eq. (50) at any point in the interior of the cube are identical to those listed in Eq. (42). This concludes the demonstration of the new hybrid method.

It is evident that the procedure used in analyzing the sample problem above is equally applicable to all other bodies that have the shape of a rectangular prism but may have very different surface stress data and sizes, as the Green function listed in Eq. (36) and the general formulas given by Eqs. (20) and (28) remain the same. This conclusion can also be extended to other three-dimensional bodies with different shapes (and thus different Green's functions), including solid cylinders and spheres whose Green functions are also provided in Section 3.

5. Summary

A new hybrid experimental–analytical/numerical method for stress analysis of a loaded finite three-dimensional elastic component is developed. This method uses experimentally measured surface stresses to analytically/numerically calculate the displacements (and thus strains and stresses) throughout the interior of the component. Assuming that the complete surface stress data could be obtained experimentally using combined thermal stress analysis and birefringent coating techniques, this paper focuses on developing the procedures for determining the displacements inside the elastic component from the known surface stresses.

The fact that the existing stress-based hybrid method is unfortunately deficient and the correct use of a stress formulation method requires solving the six Beltrami–Michell compatibility equations and the three equilibrium equations simultaneously motivates us to adopt a displacement formulation in developing the new hybrid method. As a result, only the three (independent) Navier equations need to be solved for the three unknown displacements. The first stress invariant (and thus the first strain invariant) satisfying Laplace's equation can be determined throughout the interior of the component from known surface stresses. This decouples the three Navier equations and converts them into three separate Pois-

son's equations. It then becomes possible to use standard methods in potential theory to solve elasticity problems involving finite dimensions. Green's function method is employed to solve the relevant Laplace and Poisson equations. The solutions of all these four equations are derived in integral forms in terms of the same Green function, which can be uniquely determined for given shape of the engineering component. The Green functions for three standard shapes of a rectangular prism, a solid cylinder and a solid sphere are provided here, which can represent many important cases. The general procedures given in Section 3.3 may be followed to find Green's functions for other less standard finite domains (shapes) in an approximate manner.

The sample problem of an elastic cube subjected to hydrostatic pressure is analyzed to demonstrate applications of the new method. The procedure used in this analysis is illustrative for other cases that may involve different shapes and sizes, and may have very different surface stress data.

The present hybrid method enables the determination of interior displacements (and thus stresses) at any desired locations in a loaded three-dimensional component from measured surface stresses. The formulas derived are general and can be applied to finite three-dimensional domains of arbitrary shape. Inevitably, numerical integrations are necessary in applications to three-dimensional problems with complicated shapes.

Naturally, the formulae derived here can also be directly applied to calculate the displacements in the interior of an elastic component from measured surface displacements, as is evident from the formulation in Section 3. In fact, it is easier to start from measured surface displacements than from measured surface stresses, as the step of determining the surface displacements from the known surface stresses will be eliminated. Unfortunately, the experimental determination of the full-field displacements over the surface of a three-dimensional component is not trivial.

Finally, it should be pointed out that this hybrid method differs greatly from the boundary integral equation method in elasticity, where the fundamental solution for an unbounded three-dimensional elastic body has to be applied (see, for example, Kythe, 1995, pp. 157–167). Also, this method is nondestructive and is conducted on the actual engineering component, unlike the model-based stress freezing technique in three-dimensional photoelasticity.

Acknowledgements

The material reported in this paper is based on one chapter of Xin-Lin Gao's doctoral thesis submitted to the Graduate School of the University of Wisconsin–Madison in April 1998. We thank Professor Millard W. Johnson, Jr. for helpful discussions. The authors are also very grateful to Professor C.R. Steele and one anonymous reviewer for very constructive comments on an earlier version of this paper.

Appendix A

Since we have not been able to locate any explicit proof of the well-documented fact that the six compatibility equations in terms of strain in three-dimensional elasticity are equivalent to three independent fourth-order equations (see, for example, Chou and Pagano, 1967), a proof is provided below in this appendix.

For illustration, only the Cartesian components are considered here. Note that the six Saint-Venant compatibility equations in the Cartesian coordinate system $\{x_1, x_2, x_3\} \equiv \{x, y, z\}$ are (see, for example,

Malvern, 1969, p.186)

$$\frac{\partial^2 \varepsilon_{xx}}{\partial y^2} + \frac{\partial^2 \varepsilon_{yy}}{\partial x^2} = \frac{\partial^2 \gamma_{xy}}{\partial x \partial y}, \tag{A.1a}$$

$$\frac{\partial^2 \varepsilon_{yy}}{\partial z^2} + \frac{\partial^2 \varepsilon_{zz}}{\partial y^2} = \frac{\partial^2 \gamma_{yz}}{\partial y \partial z}, \tag{A.1b}$$

$$\frac{\partial^2 \varepsilon_{zz}}{\partial x^2} + \frac{\partial^2 \varepsilon_{xx}}{\partial z^2} = \frac{\partial^2 \gamma_{zx}}{\partial z \partial x}, \tag{A.1c}$$

$$2\frac{\partial^2 \varepsilon_{xx}}{\partial y \partial z} = \frac{\partial}{\partial x}\left(- \frac{\partial \gamma_{yz}}{\partial x} + \frac{\partial \gamma_{xz}}{\partial y} + \frac{\partial \gamma_{xy}}{\partial z} \right), \tag{A.1d}$$

$$2\frac{\partial^2 \varepsilon_{yy}}{\partial z \partial x} = \frac{\partial}{\partial y}\left(\frac{\partial \gamma_{yz}}{\partial x} - \frac{\partial \gamma_{xz}}{\partial y} + \frac{\partial \gamma_{xy}}{\partial z} \right) \tag{A.1e}$$

and

$$2\frac{\partial^2 \varepsilon_{zz}}{\partial x \partial y} = \frac{\partial}{\partial z}\left(\frac{\partial \gamma_{yz}}{\partial x} + \frac{\partial \gamma_{xz}}{\partial y} - \frac{\partial \gamma_{xy}}{\partial z} \right). \tag{A.1f}$$

Taking $\partial^2/\partial z^2$ on Eq. (A.1a), $\partial^2/\partial x^2$ on Eq. (A.1b), $\partial^2/\partial y^2$ on Eq. (A.1c), $\partial^2/(\partial y \partial z)$ on Eq. (A.1d), $\partial^2/(\partial z \partial x)$ on Eq. (A.1e) and $\partial^2/(\partial x \partial y)$ on Eq. (A.1f), respectively, will yield

$$\frac{\partial^4 \varepsilon_{xx}}{\partial y^2 \partial z^2} + \frac{\partial^4 \varepsilon_{yy}}{\partial x^2 \partial z^2} = \frac{\partial^4 \gamma_{xy}}{\partial x \partial y \partial z^2}, \tag{A.2a}$$

$$\frac{\partial^4 \varepsilon_{yy}}{\partial z^2 \partial x^2} + \frac{\partial^4 \varepsilon_{zz}}{\partial y^2 \partial x^2} = \frac{\partial^4 \gamma_{yz}}{\partial y \partial z \partial x^2}, \tag{A.2b}$$

$$\frac{\partial^4 \varepsilon_{zz}}{\partial x^2 \partial y^2} + \frac{\partial^4 \varepsilon_{xx}}{\partial z^2 \partial y^2} = \frac{\partial^4 \gamma_{zx}}{\partial z \partial x \partial y^2}, \tag{A.2c}$$

$$2\frac{\partial^4 \varepsilon_{xx}}{\partial y^2 \partial z^2} = -\frac{\partial^4 \gamma_{yz}}{\partial x^2 \partial y \partial z} + \frac{\partial^4 \gamma_{xz}}{\partial x \partial y^2 \partial z} + \frac{\partial^4 \gamma_{xy}}{\partial x \partial y \partial z^2}, \tag{A.2d}$$

$$2\frac{\partial^4 \varepsilon_{yy}}{\partial z^2 \partial x^2} = \frac{\partial^4 \gamma_{yz}}{\partial x^2 \partial y \partial z} - \frac{\partial^4 \gamma_{xz}}{\partial y^2 \partial x \partial z} + \frac{\partial^4 \gamma_{xy}}{\partial x \partial y \partial z^2} \tag{A.2e}$$

and

$$2\frac{\partial^4 \varepsilon_{zz}}{\partial x^2 \partial y^2} = \frac{\partial^4 \gamma_{yz}}{\partial x^2 \partial y \partial z} + \frac{\partial^4 \gamma_{xz}}{\partial x \partial y^2 \partial z} - \frac{\partial^4 \gamma_{xy}}{\partial x \partial y \partial z^2}. \tag{A.2f}$$

Adding Eq. (A.2d) to Eq. (A.2e) gives

$$\frac{\partial^4 \varepsilon_{xx}}{\partial y^2 \partial z^2} + \frac{\partial^4 \varepsilon_{yy}}{\partial x^2 \partial z^2} = \frac{\partial^4 \gamma_{xy}}{\partial x \partial y \partial z^2}, \tag{A.3}$$

which is identical to Eq. (A.2a). Similarly, adding Eq. (A.2e) to Eq. (A.2f) leads to Eq. (A.2b), and adding Eq. (A.2f) to Eq. (A.2d) yields Eq. (A.2c). Hence, we have shown that Eqs. (A.2a), (A.2b) and (A.2c) are easily derivable from Eqs. (A.2d), (A.2e) and (A.2f). Next, we show that the converse is also true.

Adding Eq. (A.2a) to Eq. (A.2c) and then subtracting Eq. (A.2b) will yield

$$2\frac{\partial^4 \varepsilon_{xx}}{\partial y^2 \partial z^2} = \frac{\partial^4 \gamma_{xy}}{\partial x \partial y \partial z^2} + \frac{\partial^4 \gamma_{zx}}{\partial z \partial x \partial y^2} - \frac{\partial^4 \gamma_{yz}}{\partial y \partial z \partial x^2}, \tag{A.4}$$

which is just Eq. (A.2d). Similarly, adding Eq. (A.2a) to Eq. (A.2b) and then subtracting Eq. (A.2c) will give Eq. (A.2e), and adding Eq. (A.2b) to Eq. (A.2c) and then subtracting Eq. (A.2a) will lead to Eq. (A.2f). This shows that Eqs. (A.2d), (A.2e) and (A.2f) are readily obtainable from Eqs. (A.2a), (A.2b) and (A.2c).

It is therefore concluded that the first three equations in Eqs. (A.2a)–(A.2f) are equivalent to the last three equations in Eqs. (A.2a)–(A.2f). That is, there are only three independent equations among the six equations given by Eqs. (A.2a)–(A.2f). Since these six equations follow directly from Eqs. (A.1a)–(A.1f) after differentiations which are linear operations, it can be further concluded that the six compatibility equations given by Eqs. (A.1a)–(A.1f) are not independent and are equivalent to three independent fourth-order equations, i.e., Eqs. (A.2a), (A.2b) and (A.2c) or Eqs. (A.2d), (A.2e) and (A.2f). This ends our proof of the fact stated at the beginning of the appendix.

This fact, in turn, explains why the six Beltrami–Michell compatibility equations (i.e., the compatibility equations in terms of stress), which are converted from the six strain compatibility equations given by Eqs. (A.1a)–(A.1f) after some linear operations including the substitutions of the constitutive equations (and equilibrium equations), alone are insufficient, and the three equilibrium equations are required additionally, to solve for the six unknown stress components. How to solve these nine equations simultaneously should be, and has been, the starting point of any serious discussion on solving three-dimensional elasticity problems via a stress formulation method (see, for example, Chou and Pagano, 1967, pp. 277–282; Little, 1973, pp. 317–320). Unfortunately, and notwithstanding the seemingly good agreement of their results, the previous investigators mentioned in Section 1 only employed the six (dependent) Beltrami–Michell compatibility equations and omitted to enforce the three equilibrium equations in their efforts to develop a stress-based hybrid method of three-dimensional stress analysis. The enormous difficulties associated with simultaneously solving the three equilibrium equations and the six compatibility equations (or their three fourth-order equivalents) in a general context motivate us to take the other approach in developing a hybrid method of generic nature. That is,

we embark on solving the three Navior equations, which are the only governing equations in a displacement formulation, for the interior displacement field by using a Green's function method in potential theory. The required boundary data on displacements are determinable from the measured surface stresses through a suitable process involving integrations.

Appendix B

Since the derivations of the three Green functions provided in Section 3 are lengthy, we will, instead, present the proofs of their correctness in this appendix.

B.1. Proof of Green's function for a rectangular prism

To prove the correctness of the Green function given by Eq. (36) for the rectangular prism, one only needs to demonstrate that Eqs. (17a) and (17b) are identically satisfied by Eq. (36).

Note that from Eq. (36), it follows that

$$\frac{\partial^2 G}{\partial x_1^2} = 8\sum_{m=1}^{\infty}\sum_{n=1}^{\infty}\sum_{p=1}^{\infty}\frac{\sin\frac{m\pi\xi_1}{a}\sin\frac{n\pi\xi_2}{b}\sin\frac{p\pi\xi_3}{c}}{\pi^2 abc\left(\frac{m^2}{a^2}+\frac{n^2}{b^2}+\frac{p^2}{c^2}\right)}\left(\frac{m\pi}{a}\right)^2\sin\frac{m\pi x_1}{a}\sin\frac{n\pi x_2}{b}\sin\frac{p\pi x_3}{c},$$

$$\frac{\partial^2 G}{\partial x_2^2} = 8\sum_{m=1}^{\infty}\sum_{n=1}^{\infty}\sum_{p=1}^{\infty}\frac{\sin\frac{m\pi\xi_1}{a}\sin\frac{n\pi\xi_2}{b}\sin\frac{p\pi\xi_3}{c}}{\pi^2 abc\left(\frac{m^2}{a^2}+\frac{n^2}{b^2}+\frac{p^2}{c^2}\right)}\left(\frac{n\pi}{b}\right)^2\sin\frac{m\pi x_1}{a}\sin\frac{n\pi x_2}{b}\sin\frac{p\pi x_3}{c},$$

$$\frac{\partial^2 G}{\partial x_3^2} = 8\sum_{m=1}^{\infty}\sum_{n=1}^{\infty}\sum_{p=1}^{\infty}\frac{\sin\frac{m\pi\xi_1}{a}\sin\frac{n\pi\xi_2}{b}\sin\frac{p\pi\xi_3}{c}}{\pi^2 abc\left(\frac{m^2}{a^2}+\frac{n^2}{b^2}+\frac{p^2}{c^2}\right)}\left(\frac{p\pi}{c}\right)^2\sin\frac{m\pi x_1}{a}\sin\frac{n\pi x_2}{b}\sin\frac{p\pi x_3}{c}. \tag{B.1}$$

Then,

$$\Delta G = \sum_{m=1}^{\infty}\sum_{n=1}^{\infty}\sum_{p=1}^{\infty}\frac{8}{abc}\sin\frac{m\pi x_1}{a}\sin\frac{m\pi\xi_1}{a}\sin\frac{n\pi x_2}{b}\sin\frac{n\pi\xi_2}{b}\sin\frac{p\pi x_3}{c}\sin\frac{p\pi\xi_3}{c}. \tag{B.2}$$

From the distribution theory (see, for example, Stakgold, 1979; Barton, 1989),

$$\sum_{m=1}^{\infty}\frac{2}{a}\sin\frac{m\pi\xi_1}{a}\sin\frac{m\pi x_1}{a} \equiv \delta(x_1-\xi_1),\ x_1\in[0,a];$$

$$\sum_{n=1}^{\infty} \frac{2}{b} \sin \frac{n\pi\xi_2}{b} \sin \frac{n\pi x_2}{b} \equiv \delta(x_2 - \xi_2),\ x_2 \in [0,b];$$

$$\sum_{p=1}^{\infty} \frac{2}{c} \sin \frac{p\pi\xi_3}{c} \sin \frac{p\pi x_3}{c} \equiv \delta(x_3 - \xi_3),\ x_3 \in [0,c]. \tag{B.3}$$

Using Eq. (B.3) in Eq. (B.2) then gives

$$\Delta G = \delta(x_1 - \xi_1)\delta(x_2 - \xi_2)\delta(x_3 - \xi_3) \equiv \delta(\underline{x} - \underline{\xi}),\ \forall \underline{x} \in \Omega. \tag{B.4}$$

This means that Eq. (17a) is identically satisfied by the Green function given in Eq. (36). Next, note that from Eq. (36),

$$G|_{x_1=0} = 0 = G|_{x_1=a},$$

$$G|_{x_2=0} = 0 = G|_{x_2=b},$$

$$G|_{x_3=0} = 0 = G|_{x_3=c}. \tag{B.5}$$

That is, the Green function given by Eq. (36) also identically meets the boundary conditions listed in Eq. (17b). It is therefore concluded that the Green function for the rectangular prism given by Eq. (36) is indeed correct.

B.2. Proof of Green's function for a solid cylinder

In this case, one only needs to show that Eqs. (17a) and (17b) are identically satisfied by the Green function given in Eq. (37).

Note that from Eq. (37) it follows that

$$\frac{\partial}{\partial r}\left(r\frac{\partial G}{\partial r}\right) = -\sum_{m=1}^{\infty}\sum_{n=1}^{\infty} \frac{2J_0\left(\beta_m \frac{r'}{R}\right)\sin\frac{n\pi x_3}{L}\sin\frac{n\pi\xi_3}{L}}{\pi R^2 L\left[\left(\frac{\beta_m}{R}\right)^2 + \left(\frac{n\pi}{L}\right)^2\right]J_1^2(\beta_m)}\left[\frac{\beta_m}{R}J_0'\left(\beta_m\frac{r}{R}\right) + r\left(\frac{\beta_m}{R}\right)^2 J_0''\left(\beta_m\frac{r}{R}\right)\right],$$

$$\frac{\partial^2 G}{\partial\theta^2} = 0,$$

$$\frac{\partial^2 G}{\partial x_3^2} = \sum_{m=1}^{\infty}\sum_{n=1}^{\infty} \frac{2}{\pi R^2 L\left[\left(\frac{\beta_m}{R}\right)^2+\left(\frac{n\pi}{L}\right)^2\right]} \frac{J_0\left(\beta_m\frac{r}{R}\right)J_0\left(\beta_m\frac{r'}{R}\right)}{J_1^2(\beta_m)}\left(\frac{n\pi}{L}\right)^2 \sin\frac{n\pi x_3}{L}\sin\frac{n\pi\xi_3}{L}. \tag{B.6}$$

Then,

$$\begin{aligned}\Delta G = &-\sum_{m=1}^{\infty}\sum_{n=1}^{\infty} \frac{2}{\pi R^2 L\left[\left(\frac{\beta_m}{R}\right)^2+\left(\frac{n\pi}{L}\right)^2\right]} \frac{J_0\left(\beta_m\frac{r'}{R}\right)}{J_1^2(\beta_m)}\sin\frac{n\pi x_3}{L}\sin\frac{n\pi\xi_3}{L}\\ &\times\left[\left(\frac{\beta_m}{R}\right)^2 J_0''\left(\beta_m\frac{r}{R}\right)^2+\frac{\beta_m}{rR}J_0'\left(\beta_m\frac{r}{R}\right)-\left(\frac{n\pi}{L}\right)^2 J_0\left(\beta_m\frac{r}{R}\right)\right].\end{aligned} \tag{B.7}$$

By definition, $J_0(x)$ must satisfy the Bessel equation of order 0 (see, for example, Andrews, 1992, p.243):

$$\frac{\mathrm{d}^2 J_0}{\mathrm{d}x^2}+\frac{1}{x}\frac{\mathrm{d}J_0}{\mathrm{d}x}+J_0=0. \tag{B.8}$$

Using Eq. (B.8) in Eq. (B.7) then gives

$$\Delta G = \sum_{m=1}^{\infty}\sum_{n=1}^{\infty} \frac{2}{\pi R^2 L}\frac{J_0\left(\beta_m\frac{r'}{R}\right)J_0\left(\beta_m\frac{r}{R}\right)}{J_1^2(\beta_m)}\sin\frac{n\pi x_3}{L}\sin\frac{n\pi\xi_3}{L}. \tag{B.9}$$

Next, note that $J_0(x)$ also satisfies the following orthogonality relations (see, for example, Andrews, 1992, pp. 267–273):

$$\int_0^b xJ_0(k_m x)J_0(k_n x)\mathrm{d}x = 0 \ (m\neq n),$$

$$\int_0^b x[J_0(k_m x)]^2\mathrm{d}x = \frac{1}{2}b^2[J_1(k_m b)]^2 \ (m=n), \tag{B.10}$$

where k_m and k_n are dimensionless distinct roots of $J_0(kb)=0$, and b is some positive real number. By using Eq. (B.10), $\delta(r-r')$ can then be expanded as a Fourier–Bessel series of the following form:

$$\delta(r-r') = \sum_{m=1}^{\infty}\frac{2r'}{R^2}\frac{J_0\left(\beta_m\frac{r'}{R}\right)J_0\left(\beta_m\frac{r}{R}\right)}{J_1^2(\beta_m)}, \ \forall r\in[0,R]. \tag{B.11}$$

With the help of Eqs. (B.3) and (B.11), Eq. (B.9) now becomes

$$\Delta G = \frac{1}{2\pi r'}\delta(r-r')\delta(x_3-\xi_3) = \delta(x_1-\xi_1)\delta(x_2-\xi_2)\delta(x_3-\xi_3) \equiv \delta(\underline{x}-\underline{\xi}),\ \forall \underline{x} \in \Omega, \tag{B.11}$$

where the second equality is based on one property of the Dirac delta function (see, for example, Barton, 1989, pp. 7–37). This shows that the Green function given by Eq. (37) does satisfy Eq. (17a) identically. Next, note that from Eq. (37),

$$G|_{r=R} = 0, \quad G|_{x_3=0} = 0 = G|_{x_3=L}, \tag{B.13}$$

where use has been made of the fact $J_0(b_m)=0$ in reaching the first equality. Eq. (B.13) says that the Green function given by Eq. (37) also identically meets the boundary conditions listed in Eq. (17b). Hence, we have proven that the Green function given by Eq. (37) for the solid cylinder is indeed correct.

B.3. Proof of Green's function for a solid sphere

Similarly, in this case one only needs to prove that Eqs. (17a) and (17b) are identically satisfied by the Green function given in Eq. (38).

Note that from Eq. (38) it follows that

$$\frac{\partial}{\partial r}\left(r^2\frac{\partial G}{\partial r}\right) = \sum_{m=1}^{\infty}\frac{r}{2\pi R r'}\sin\frac{m\pi r'}{R}\sin\frac{m\pi r}{R},\ \frac{\partial G}{\partial \theta} = 0,\ \frac{\partial^2 G}{\partial \varphi^2} = 0. \tag{B.14}$$

Then,

$$\Delta G = \sum_{m=1}^{\infty}\frac{1}{2\pi R r r'}\sin\frac{m\pi r'}{R}\sin\frac{m\pi r}{R}. \tag{B.15}$$

With the help of Eq. (B.3), Eq. (B.15) reduces to

$$\Delta G = \frac{1}{4\pi r r'}\delta(r-r') = \delta(\underline{r}-\underline{r}') \equiv \delta(\underline{x}-\underline{\xi}),\ \forall \underline{x} \in \Omega, \tag{B.16}$$

where the second equality is based on one property of the Dirac delta function (see, for example, Barton, 1989, pp. 7–37). Eq. (B.16) shows that the Green function given by Eq. (38) does satisfy Eq. (17a) identically. Next, note that from Eq. (38),

$$G|_{r=R} = 0. \tag{B.17}$$

That is, the Green function given by Eq. (38) also identically meets the boundary conditions listed in Eq. (17b). Therefore, it is concluded that the Green function given by Eq. (38) for the solid sphere is indeed correct.

Appendix C

Since the determination of the surface displacements from the measured surface stresses (and thus the surface strains by Hooke's law) is an important step in the new hybrid method, the derivation of the three displacement components given by Eq. (42) from the six strain components listed in Eq. (41) is recorded in details in this appendix to illustrate the procedure.

Substituting Eq. (41) into Eq. (3) leads to

$$\frac{\partial u_1}{\partial x_1} = -\frac{q(1-2\nu)}{E}, \tag{C.1a}$$

$$\frac{\partial u_2}{\partial x_2} = -\frac{q(1-2\nu)}{E}, \tag{C.1b}$$

$$\frac{\partial u_3}{\partial x_3} = -\frac{q(1-2\nu)}{E}, \tag{C.1c}$$

$$\frac{\partial u_1}{\partial x_2} + \frac{\partial u_2}{\partial x_1} = 0, \tag{C.1d}$$

$$\frac{\partial u_1}{\partial x_3} + \frac{\partial u_3}{\partial x_1} = 0 \tag{C.1e}$$

and

$$\frac{\partial u_2}{\partial x_3} + \frac{\partial u_3}{\partial x_2} = 0 \tag{C.1f}$$

at any $\underline{x} \in \Omega \cup \Gamma$. Since the strain components given by Eq. (41) identically satisfy the compatibility equations listed in Eq. (4), it is guaranteed that the six equations in Eqs. (C.1a)–(C.1f) can be solved to obtain the three displacements $u_i(\underline{x})$, as discussed at the beginning of Section 3.2. We will use the direct integration approach mentioned there (see also Gao, 1999 for one example using the polar coordinate system) in our derivation to follow.

From Eq. (C.1a), it follows that

$$u_1 = -\frac{q(1-2\nu)}{E}x_1 + f(x_2,x_3), \tag{C.2}$$

where $f(x_2, x_3)$ is a yet-unknown function. Using Eq. (C.2) in Eqs. (C.1d) and (C.1e) gives

$$u_2 = -\frac{\partial f}{\partial x_2}x_1 + g(x_2,x_3), \quad u_3 = -\frac{\partial f}{\partial x_3}x_1 + h(x_2,x_3), \tag{C.3}$$

where $g(x_2, x_3)$ and $h(x_2, x_3)$ are two additional unknown functions. Next, substituting Eq. (C.3) into Eqs. (C.1b) and (C.1c) yields

$$-\frac{\partial^2 f}{\partial x_2^2}x_1 + \frac{\partial g}{\partial x_2} = -\frac{q(1-2\nu)}{E}, \quad -\frac{\partial^2 f}{\partial x_3^2}x_1 + \frac{\partial h}{\partial x_3} = -\frac{q(1-2\nu)}{E} \tag{C.4}$$

at any $\underline{x} \in \Omega \cup \Gamma$, which imply that

$$\frac{\partial^2 f}{\partial x_2^2} \equiv 0, \tag{C.5a}$$

$$\frac{\partial^2 f}{\partial x_3^2} \equiv 0, \tag{C.5b}$$

$$\frac{\partial g}{\partial x_2} \equiv -\frac{q(1-2\nu)}{E} \tag{C.5c}$$

and

$$\frac{\partial h}{\partial x_3} \equiv -\frac{q(1-2\nu)}{E}. \tag{C.5d}$$

From Eqs. (C.5c) and (C.5d), it follows that

$$g(x_2,x_3) = -\frac{q(1-2\nu)}{E}x_2 + G(x_3),\ h(x_2,x_3) = -\frac{q(1-2\nu)}{E}x_3 + H(x_2), \tag{C.6}$$

where $G(x_3)$ and $H(x_2)$ are two yet-unknown functions. Using Eq. (C.6) in Eq. (C.3) gives

$$u_2 = -\frac{\partial f}{\partial x_2}x_1 - \frac{q(1-2\nu)}{E}x_2 + G(x_3),$$

$$u_3 = -\frac{\partial f}{\partial x_3}x_1 - \frac{q(1-2\nu)}{E}x_3 + H(x_2). \tag{C.7}$$

Inserting Eq. (C.7) into Eq. (C.1f), the only remaining equation in Eqs. (C.1a)–(C.1f) yields

$$-2\frac{\partial^2 f}{\partial x_2 \partial x_3}x_1 + G'(x_3) + H'(x_2) = 0 \tag{C.8}$$

at any $\underline{x} \equiv (x_1, x_2, x_3) \in \Omega \cup \Gamma$, which suggests that

$$\frac{\partial^2 f}{\partial x_2 \partial x_3} \equiv 0 \tag{C.9a}$$

and

$$G'(x_3) = -H'(x_2) \equiv C, \tag{C.9b,c}$$

with C being a constant. From Eqs. (C.5a), (C.5b) and (C.9a), it immediately follows that

$$f(x_2,x_3) = Dx_2 + Fx_3 + K, \tag{C.10}$$

and from Eqs. (C.9b,c) that

$$G(x_3) = Cx_3 + M,\ H(x_2) = -Cx_2 + N, \tag{C.11}$$

where D, F, K, M and N are additional constants. Using Eqs. (C.10) and (C.11) in Eqs. (C.2) and (C.7) then gives

$$u_1(\underline{x}) = -\frac{q(1-2\nu)}{E}x_1 + Dx_2 + Fx_3 + K,$$

$$u_2(\underline{x}) = -\frac{q(1-2\nu)}{E}x_2 + Cx_3 - Dx_1 + M,$$

$$u_3(\underline{x}) = -\frac{q(1-2\nu)}{E}x_3 - Cx_2 - Fx_1 + N \tag{C.12}$$

as the displacements at any point $\underline{x} \in \Omega \cup \Gamma$. Clearly, the last three terms in each of the three displacements given by Eq. (C.12) represent the contributions of a rigid-body motion. These terms have no effects on the strain and stress distributions (see, for example, Chou and Pagano, 1967, pp. 45–48) and can therefore be suppressed without violating any stress boundary conditions. For example, if we assume that the origin $O(0,0,0)$, which happens to be a point on the surface, is fixed, i.e., $u_1 = u_2 = u_3 = 0$ at $x_1 = x_2 = x_3 = 0$, then it follows from Eq. (C.12) that

$$K = M = N = 0. \tag{C.13}$$

This condition suppresses all possible rigid-body translations of the cube. Next, if we impose that the cube does not have any rigid-body rotation, i.e.,

$$\omega_1 = \frac{1}{2}\left(\frac{\partial u_3}{\partial x_2} - \frac{\partial u_2}{\partial x_3}\right) = 0,$$

$$\omega_2 = \frac{1}{2}\left(\frac{\partial u_1}{\partial x_3} - \frac{\partial u_3}{\partial x_1}\right) = 0,$$

$$\omega_3 = \frac{1}{2}\left(\frac{\partial u_2}{\partial x_1} - \frac{\partial u_1}{\partial x_2}\right) = 0, \tag{C.14}$$

then it follows from Eqs. (C.12) and (C.14) that

$$C = D = F = 0. \tag{C.15}$$

The substitution of Eqs. (C.13) and (C.15) into Eq. (C.12) finally yields

$$u_1(\underline{x}) = -\frac{q(1-2\nu)}{E}x_1,$$

$$u_2(\underline{x}) = -\frac{q(1-2\nu)}{E}x_2,$$

$$u_3(\underline{x}) = -\frac{q(1-2\nu)}{E}x_3 \tag{C.16}$$

as the displacement components at any point $\underline{x} \in \Omega \cup \Gamma$ with the rigid-body motion suppressed, which are the very expressions listed in Eq. (42).

References

Andrews, L.C., 1992. Special Functions of Mathematics for Engineers. McGraw–Hill, New York.

Barishpolsky, B.M., 1980. A combined experimental and numerical method for the solution of generalized elasticity problems. Exp. Mech. 20, 345–349.

Barishpolsky, B.M., 1981. Development of a combined experimental and numerical method for the thermoelastic analysis. In: Proc. 1981 SESA Spring Meeting, pp. 25–30.

Barone, S., Wang, Z.F., Patterson, E.A., 1998. Automated photoelasticity applied with thermoelasticity to real components. In: Lagarde, A. (Ed.), Proc. IUTAM Symposium on Advanced Optical Methods and Applications in Solid Mechanics, vol. 2, pp. 1–8, Aug. 31–Sept. 4, 1998, Poitiers, France.

Barton, G., 1989. Elements of Green's Functions and Propagation: Potentials, Diffusion, and Waves. Clarendon, Oxford.

Chandrashekhara, K., Jacob, K.A., 1977a. An experimental–numerical hybrid technique for two-dimensional stress analysis. Strain 13, 25–28.

Chandrashekhara, K., Jacob, K.A., 1977b. An experimental–numerical hybrid technique for three dimensional stress analysis. Int. J. Numerical Methods in Engineering 11, 1845–1863.

Chou, P.C., Pagano, N.J., 1967. Elasticity–Tensor, Dyadic, and Engineering Approaches. D. Van Nostrand, Princeton, NJ.

Flanigan, F.J., 1972. Complex Variables: Harmonic and Analytic Functions. Allyn and Bacon, Boston.

Gao, X.-L., 1999. An exact elasto–plastic solution for the plane wedge problem of an elastic linear-hardening material. Math. Mech. Solids 4, 289–306.

Jacob, K.A., 1976. An experimental–numerical hybrid technique for two and three dimensional stress analysis. Ph.D. Dissertation, Indian Institute of Science, Bangalore, India.

Kellogg, O.D., 1953. Foundations of Potential Theory. Dover, New York.

Kythe, P.K., 1995. An Introduction to Boundary Element Methods. CRC Press, Boca Raton, FL.

Laermann, K.H., 1984a. Reconstruction of the internal state of displacement in solids from boundary values. Mech. Res. Communications 11, 137–143.

Laermann, K.H., 1984b. Reconstruction of internal stress and strain state from boundary displacements. In: Proc. 5th Int. Cong. Exp. Mech, pp. 204–208, June 10–15, 1984, Montreal.

Laermann, K.H., 1990. On a method to analyze the internal stress–strain-state in three-dimensional solids. J. Struc. Engng. 16, 115–121.

Lesniak, J.R., Zickel, M.J., Welch, C.S., Johnson, D.F., 1997. An innovative polariscope for photoelastic stress analysis. In: Proc. 1997 SEM Spring Conference on Experimental Mechanics, pp. 219–224, June 2–4, 1997, Bellevue, Washington, USA.

Little, R., 1973. Elasticity. Prentice–Hall, Englewood Cliffs, NJ.

Love, A.E.H., 1944. A Treatise on the Mathematical Theory of Elasticity. Cambridge University Press, Cambridge.

Malvern, L.E., 1969. Introduction to the Mechanics of a Continuous Medium. Prentice–Hall, Englewood Cliffs, NJ.

Rao, G.V., 1982. Experimental–numerical hybrid techniques for body-force and thermal stress problems — Applications in power industry. In: Proc. 1982 Conf. Exp. Mech., SESA, pp. 398–404.

Rauch, B.J., Rowlands, R.E., 1993. Thermoelastic stress analysis. In: Kobayashi, A.S. (Ed.), Handbook on Experimental Mechanics, 2nd ed. VCH Publishers, New York, pp. 581–599.

Rowlands, R.E., 1981. Applications of photoelastic coatings to composites. In: Holister, G.S. (Ed.), Developments in Composite Materials, vol. 2. Applied Science Publishers, London, pp. 101–134.

Sneddon, I.N., 1966. Mixed Boundary Value Problems in Potential Theory. North–Holland, Amsterdam.

Sokolnikoff, I.S., 1956. Mathematical Theory of Elasticity, 2nd ed. McGraw–Hill, New York.

Stakgold, I., 1979. Green's Functions and Boundary Value Problems. Wiley, New York.

Zandman, F., Redner, S., Dally, J.W., 1977. Photoelastic Coatings. Iowa State University Press, Ames, Iowa.